

The TOR and EGO Protein Complexes Orchestrate Microautophagy in Yeast

Frédérique Dubouloz, Olivier Deloche,
Valeria Wanke, Elisabetta Cameroni,
and Claudio De Virgilio*

Department of Microbiology and Molecular Medicine
University of Geneva Medical School
1211 Geneva 4
Switzerland

Summary

The rapamycin-sensitive TOR signaling pathway in *Saccharomyces cerevisiae* positively controls cell growth in response to nutrient availability. Accordingly, TOR depletion or rapamycin treatment causes regulated entry of cells into a quiescent growth phase. Although this process has been elucidated in considerable detail, the transition from quiescence back to proliferation is poorly understood. Here, we describe the identification of a conserved member of the RagA subfamily of Ras-related GTPases, Gtr2, which acts in a vacuolar membrane-associated protein complex together with Ego1 and Ego3 to ensure proper exit from rapamycin-induced growth arrest. We demonstrate that the EGO complex, in conjunction with TOR, positively regulates microautophagy, thus counterbalancing the massive rapamycin-induced, macroautophagy-mediated membrane influx toward the vacuolar membrane. Moreover, large-scale genetic analyses of the EGO complex confirm the existence of a growth control mechanism originating at the vacuolar membrane and pinpoint the amino acid glutamine as a key metabolite in TOR signaling.

Introduction

The highly conserved target of rapamycin (TOR) proteins control cell proliferation in yeast, flies, and mammalian cells in response to growth factors and/or nutrients (Jacinto and Hall, 2003). *S. cerevisiae* cells express two TOR homologs, Tor1 and Tor2, both of which—when associated with Lst8 and Kog1 in the TORC1 complex—are targets of the therapeutically important, immune-suppressive macrolide rapamycin in complex with the peptidyl-prolyl isomerase Fpr1 (also known as FK506 binding protein [FKBP] in mammals) (Jacinto and Hall, 2003; Loewith et al., 2002). Binding of the rapamycin-FKBP complex to TORC1, a mode of action that is conserved from yeast to human (Hara et al., 2002; Kim et al., 2002), inhibits the activity of the TOR kinases and elicits a number of responses that mimic nutrient starvation, including a decrease of protein synthesis and ribosome biogenesis, specific changes in gene transcription, sorting and turnover of nutrient permeases, induction of autophagy, cell cycle arrest at the G₁/S boundary, and entry into G₀ (Jacinto and Hall, 2003). Downstream of TORC1, many processes are reg-

ulated by the type 2A (Pph21 and Pph22) or type 2A-related (Sit4) protein phosphatases (PP2As) and the regulatory proteins Tap42 and Tip41 (Düvel and Broach, 2004). For instance, rapamycin treatment causes activation of the GATA-type transcription factors Gln3 and Gat1 via modulation of Tap42, thereby inducing (among others) the expression of the nitrogen discrimination pathway (NDP) genes, whose products serve to assimilate alternative nitrogen sources (e.g., proline and allantoin) and to synthesize glutamine (Cooper, 2002). In addition, rapamycin-induced, Sit4-dependent dephosphorylation results in activation of the Npr1 protein kinase, which in turn induces degradation of the high-affinity tryptophan permease Tat2 (Schmidt et al., 1998).

TOR has been postulated to act as a multichannel processor that integrates different nutritional signals (Shamji et al., 2000). However, the putative nutrient metabolites that activate TOR signaling still remain elusive, although some evidence exists suggesting that certain amino acids, specifically glutamate and glutamine, may be important nutrients in TOR signaling (Crespo et al., 2002; Komeili et al., 2000; Shamji et al., 2000). Both glutamate and glutamine are key intermediates in nitrogen metabolism that can readily be converted to α -ketoglutarate (for use in TCA cycle) or serve as immediate precursors for the biosynthesis of other amino acids, nucleotides and nitrogen-containing molecules, such as NAD⁺ (Magasanik and Kaiser, 2002). Starvation for glutamine results in a phenotype similar to TOR inactivation, inasmuch as it causes nuclear localization and activation of Gln3 and of the heterodimeric transcription factor Rtg1/Rtg3, which in turn activates genes whose products (e.g., mitochondrial and peroxisomal enzymes) are required for biosynthesis and homeostasis of glutamate and glutamine (Butow and Avadhani, 2004; Crespo et al., 2002). Both Rtg1 and Rtg3, as well as the upstream regulatory Rtg2 protein, were originally identified as mediators of a mitochondria-to-nucleus signaling pathway, or retrograde response pathway, that senses the functional state of mitochondria via the level of glutamate and/or glutamine (Butow and Avadhani, 2004). These findings underline the potential importance of glutamine in TOR signaling, although it is not clear whether TOR signaling and retrograde regulation constitute distinct pathways that converge on Rtg1/Rtg3 or whether they are part of the same pathway (Butow and Avadhani, 2004; Crespo et al., 2002; Tate and Cooper, 2003).

An important aspect of cellular fitness under conditions of TOR inactivation and/or nutrient starvation is the capacity to ensure the production of essential proteins, which is achieved in part by downregulation of general (but not specific) protein synthesis. Accordingly, TOR depletion or rapamycin treatment results in the destabilization of the initiation factor eIF4G, inhibition of ribosome biogenesis, and activation of the highly conserved Gcn2 protein kinase via a Tap42-dependent mechanism (Cherkasova and Hinnebusch, 2003; Jacinto and Hall, 2003). Once activated, Gcn2 stimulates phosphorylation of the α subunit of the

*Correspondence: claudio.devirgilio@medecine.unige.ch

translation initiation factor 2 (eIF2 α), thereby slowing the rate of GDP-GTP exchange on eIF2. This process reduces the overall translation initiation rate, yet specifically favors translation of the *GCN4* mRNA, which encodes a transactivator of amino acid biosynthetic genes (Hinnebusch, 1997). Under conditions of TOR depletion, translation of such critical factors as Gcn4 is accomplished by regeneration of internal nutrient pools via macroautophagic recycling of cytoplasmic material (Jacinto and Hall, 2003; Levine and Klionsky, 2004).

The pathways that regulate entry of cells into a quiescent growth phase as a result of downregulation of TOR and/or nutrient starvation are understood in considerable detail, yet the mechanisms that control the transition from quiescence back to proliferation have received surprisingly little attention thus far (Gray et al., 2004). Here, we describe the discovery of a vacuolar membrane associated protein complex, which plays an essential function in exit from rapamycin-induced growth arrest: the EGO complex. We demonstrate that the EGO complex, in conjunction with TOR, positively regulates microautophagy. This process, which counterbalances the massive rapamycin-induced, macroautophagy-mediated membrane influx toward the vacuolar membrane, is essential for resumption of growth following rapamycin treatment.

Results

Exit from Rapamycin-Induced Growth Arrest: A Functional Profile of the Yeast Genome

To identify genes whose products are involved in exit from rapamycin-induced growth arrest, we individually screened (in duplicate) 4857 viable yeast deletion mutants for a defect in resumption of growth following rapamycin treatment (see Experimental Procedures). A total of eight mutants were recovered in this screen: three of these were defective in phospholipid and amino acid metabolism (i.e., *pib2* Δ , *sac3* Δ , and *hom2* Δ), one in molecular chaperone activity (*vdj1* Δ), and one in an as-yet-unidentified cellular process (*vd1172c* Δ). The remaining three mutants (*ykr007w* Δ /*meh1* Δ /*ego1* Δ , *gtr2* Δ , and *ybr077c* Δ /*ego3* Δ) were grouped in a separate class based on our findings that the corresponding gene products act in a common protein complex as assayed by both two-hybrid (Figure 1A) and coprecipitation analyses (Figure 1B). Notably, the *ykr007w* Δ /*meh1* Δ /*ego1* Δ , *gtr2* Δ , and *ybr077c* Δ /*ego3* Δ mutants normally responded to rapamycin treatment by transcriptional induction of a characteristic set of stress response genes (e.g., *HSP12*, *HSP26*, and *GRE1*; Figure 2A), transcriptional repression of *SSB1* (Figure 2A), accumulation of glycogen (Figure 2B), induction of macroautophagy (Figures 2C and 2D), and inhibition of protein synthesis (Figures 2E and 2F). Thus, by several criteria, the three mutants normally enter into the rapamycin-induced growth arrest program. Importantly, despite their defect in recovery from rapamycin treatment (Figure 2G), the *ykr007w* Δ /*meh1* Δ /*ego1* Δ , *gtr2* Δ , and *ybr077c* Δ /*ego3* Δ mutants did not significantly lose viability (as assayed by trypan blue exclusion experiments) during the rapamycin treatment and during at least the first 48 hr following rapamycin release (data

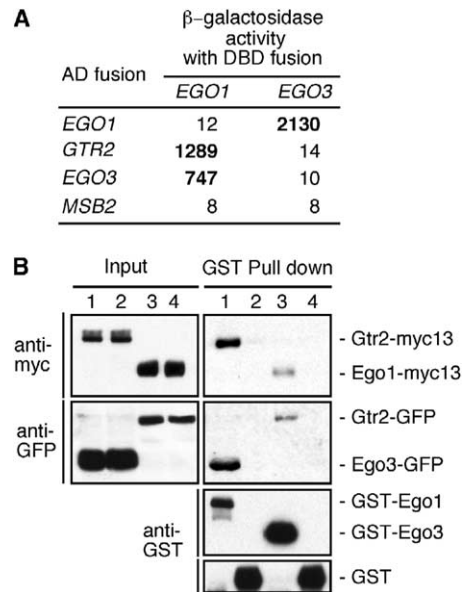


Figure 1. Ego1, Gtr2, and Ego3 Are Constituents of the EGO Protein Complex

(A) Two-hybrid interactions between Ego1, Gtr2, and Ego3. β -Galactosidase activities were measured in three independent isolates of each strain after growth for 16 hr at 30°C in SGal/Raf medium. The average values (in Miller units) are shown. Values that are at least tenfold higher than the corresponding control (*MSB2*) are shown in boldface.

(B) Coprecipitation of Ego1, Gtr2, and Ego3. Strain FD24 expressing genomically tagged Gtr2-myc13 and Ego3-GFP was transformed with pCDV1084, which expresses *GST-EGO1* under the control of the *ADH1* promoter (lane 1), or with a control plasmid (pCDV1082; *ADH1-GST*; lane 2). To independently confirm the coprecipitation of the three proteins, strain FD25 expressing genomically tagged Ego1-myc13 and Gtr2-GFP was transformed with pCDV1083, which expresses *GST-EGO3* under the control of the *ADH1* promoter (lane 3), or with a control plasmid (pCDV1082; *ADH1-GST*; lane 4). Cell lysates (Input) and GST pull-down fractions were subjected to PAGE and immunoblots were probed using anti-myc, anti-GFP, or anti-GST antibodies as indicated.

not shown). These results, together with our observation that rapamycin-induced inhibition of protein synthesis (as assayed by both incorporation of radioactively labeled amino acids into TCA precipitable material [Figure 2E; and data not shown] and phosphorylation of eIF2 α on Ser 51 [Figure 2F]) could be reversed in wild-type cells, but not in the *ykr007w* Δ /*meh1* Δ /*ego1* Δ , *gtr2* Δ , and *ybr077c* Δ /*ego3* Δ mutants, argue strongly that the corresponding three proteins are essential for resumption of growth following rapamycin treatment. For the remainder of the text, we will refer to Ykr007W/Meh1/Ego1 as Ego1, Ybr077C/Ego3 as Ego3, and the protein complex containing Ego1, Gtr2, and Ego3 as the EGO complex.

The EGO Complex Harbors a Member of the RagA Subfamily of Ras-Related GTPases

Gtr2 has previously been described as a member of a new G protein family that includes its yeast homolog Gtr1 and the mammalian RagA, -B, -C, and -D (Naka-

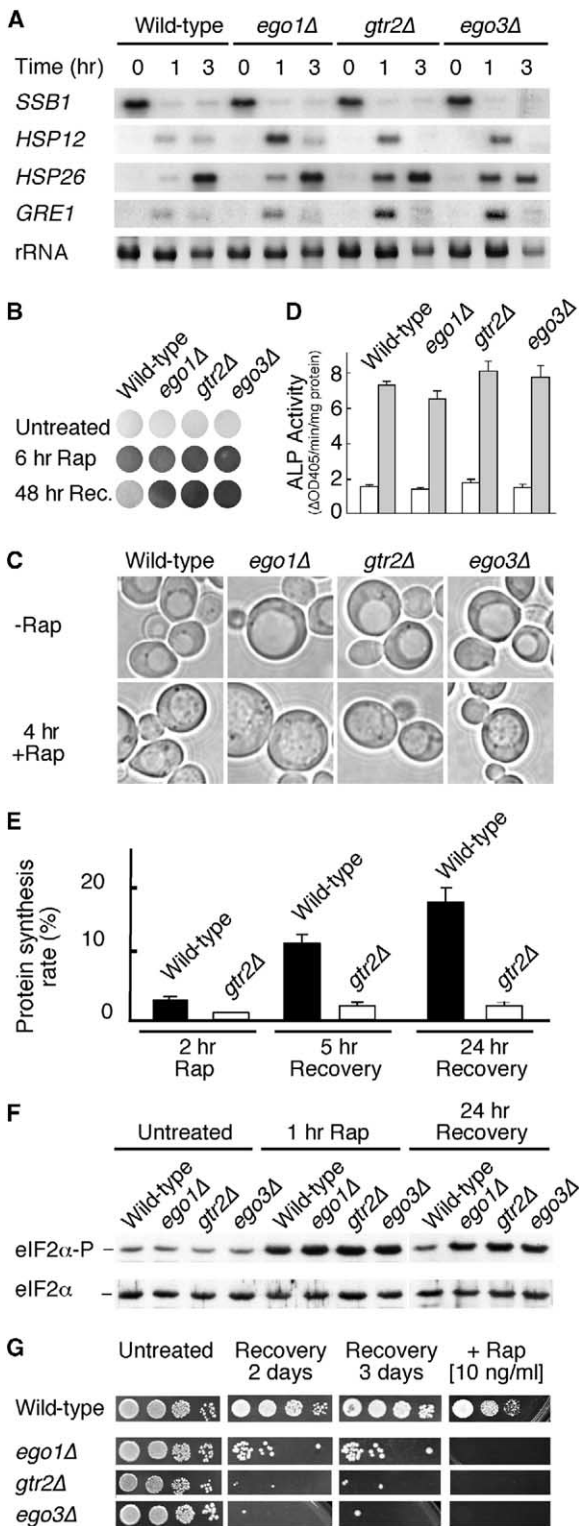


Figure 2. The EGO Complex Is Essential for Exit from, but Not Entry into, the Rapamycin-Induced Growth Arrest Program

(A) Northern analysis of indicated genes; (B) glycogen levels (visualized after exposure for 1 min to iodine vapor); and (C) microscopic analysis of macroautophagy (in the presence of 1 mM PMSF to prevent vacuolar degradation of autophagic bodies) of exponentially growing wild-type (KT1960) and isogenic *ego1Δ* (CDV210),

shima et al., 1999; Sekiguchi et al., 2001). While the specific function of these proteins is still unknown, genetic studies have implicated Gtr2 in the control of the Ran/Gsp1-GTPase, which plays a prominent role in nuclear trafficking of macromolecules (Nakashima et al., 1999). To investigate the function of Gtr2, we mutated the conserved Glu (Q) 66 residue to Leu (L), which—in analogy with the paradigmatic Ras mutations that lead to oncogenic transformation (Boguski and McCormick, 1993)—should result in a GTPase-deficient, constitutively GTP bound Gtr2^{Q66L} protein. Interestingly, unlike wild-type Gtr2, the Gtr2^{Q66L} variant did not complement the defect for exit from rapamycin-induced growth arrest of *gtr2Δ* cells (Figure 3A) and caused a defect in recovery from rapamycin treatment and rapamycin hypersensitivity when expressed in wild-type cells (Figures 3A and 3B). This dominant negative phenotype could result from the failure of the presumably GTP-locked Gtr2^{Q66L} protein to effectively release a critical downstream effector and indicates that Gtr2 may function as a small GTPase that becomes essential for growth under conditions of diminished TORC1 activity. In support of this notion, we found that loss of Gtr2, like loss of Ego1 and Ego3, resulted in pronounced rapamycin hypersensitivity (Figures 2G and 3C). Moreover, since overproduction of either Gtr2, or Ego3 conferred significantly enhanced resistance to rapamycin treatment (Figure 3D), our data indicate that the EGO complex functions in the rapamycin-sensitive TORC1 network.

gtr2Δ (CDV212), and *ego3Δ* (CDV211) mutant cells following treatment with rapamycin (200 ng/ml) for the times indicated. (D) Wild-type (TS139), *ego1Δ* (CDV284), *gtr2Δ* (CDV286), and *ego3Δ* (CDV285) cells (all expressing the modified alkaline phosphatase form Pho8Δ60) were grown exponentially and treated for 6 hr with rapamycin (200 ng/ml; gray bars) or the drug vehicle alone (white bars) and then subjected to the alkaline phosphatase (autophagy) assay. Data represent mean ± SD (n = 4). (E) Protein synthesis rates were measured in wild-type (KT1960) and *gtr2Δ* (CDV212) mutant cells following a 2 hr rapamycin treatment (200 ng/ml) and after recovery (for either 5 or 24 hr) from a 6 hr rapamycin treatment and expressed in % of the protein synthesis rate in corresponding untreated exponentially growing cells. Protein synthesis rates in exponentially growing wild-type and *gtr2Δ* cells were essentially the same. Data represent mean ± SD (n = 4). (F) Reversal of rapamycin-induced eIF2α phosphorylation (on Ser 51) during recovery from rapamycin treatment requires the presence of Ego1, Gtr2, and Ego3. Wild-type, *ego1Δ*, *gtr2Δ*, and *ego3Δ* cells (same strains as in A–C) were grown and treated as in (E). Whole cell extracts were prepared prior to rapamycin treatment (exponentially growing cells; untreated), after a 1 hr rapamycin treatment, and after recovery for 24 hr from a 6 hr rapamycin treatment. Phosphorylation of Ser 51 in eIF2α was detected by immunoblot analysis with antibodies specific for eIF2α phosphorylated on Ser 51 (eIF2α-P) and compared with the total amount of eIF2α detected with antibodies against eIF2α. (G) Behavior of *ego1Δ*, *gtr2Δ*, and *ego3Δ* mutants with a defect in recovery from rapamycin treatment. Exponentially growing wild-type (BY4741) and isogenic YKO mutant cells (OD₆₀₀ of 1.0) were treated for 6 hr with rapamycin (200 ng/ml), washed twice, resuspended in YPD without rapamycin, and spotted on YPD plates. Spots (4 μl) correspond to serial 10-fold dilutions of equally dense cultures (i.e., the first spot in each column results from a culture with an OD₆₀₀ of 1.0). In control experiments, the same exponentially growing, but untreated cultures were directly spotted on YPD plates (untreated) or on YPD plates containing a subinhibitory concentration of rapamycin (+Rap [10 ng/ml]). Cells were grown on YPD (A–G).

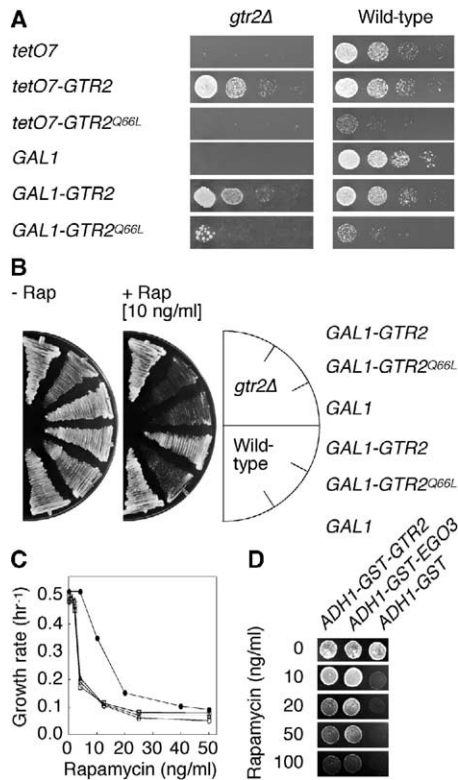


Figure 3. The EGO Complex Functions in the TORC1 Signaling Network

(A and B) Expression of Gtr2^{Q66L} mutant protein results in a dominant-negative rapamycin hypersensitivity phenotype. Expression of the Gtr2^{Q66L} (but not of Gtr2) protein from the *tetO7* or *GAL1* promoter fails to complement the recovery defect following a 6 hr rapamycin treatment in *gtr2Δ* cells (A), strongly reduces the ability of wild-type cells to recover from a 6 hr rapamycin treatment (A), and results in rapamycin hypersensitivity (B). Wild-type (KT1960) and *gtr2Δ* (CDV212) cells bearing *tetO7* (pCM189), *tetO7-GTR2* (pVW1009), *tetO7-GTR2^{Q66L}* (pVW1010), or *GAL1* (YCpIF2) on centromeric plasmids, or else *GAL1-GTR2* (pCDV991) and *GAL1-GTR2^{Q66L}* (pCDV992) integrated at the *LEU2* locus, were pregrown overnight on SD or SGal/Raf to induce expression from either the *tetO7* or *GAL1* promoter, respectively. Subsequently, cells were either subjected to a 6 hr rapamycin treatment, washed, resuspended, and spotted on YPD plates as in Figure 2G (A) or directly streaked on YPD plates containing either no (– Rap), or a subinhibitory amount of rapamycin (+ Rap [10 ng/ml]) (B). Plates were incubated for 2 days at 30°C.

(C) EGO complex mutants are hypersensitive to rapamycin. Growth rates of wild-type (●), *ego1Δ* (□), *gtr2Δ* (○), and *ego3Δ* (△) YKO strains are shown as a function of the rapamycin concentration in the medium (YPD).

(D) Overexpression of either *GTR2* or *EGO3* from the strong constitutive *ADH1* promoter confers enhanced rapamycin resistance. Wild-type cells (CDV147) carrying either the integrative plasmid pCDV1080 (*ADH1-GST-GTR2*), pCDV1083 (*ADH1-GST-EGO3*), or a corresponding control plasmid (pCDV1082; *ADH1-GST*) were grown on SD medium to an equal density (OD₆₀₀ of 2.0), spotted (4 μl) on YPD plates that contained either no—or the indicated amount of—rapamycin, and incubated for 4 days at 30°C.

The EGO Complex Localizes to the Vacuolar Membrane

Based on our biochemical and genetic results, we anticipated that the localization of Ego1, Gtr2, and Ego3

should overlap in the cell. To test this prediction, the chromosomal copies of *EGO1*, *GTR2*, and *EGO3* were fused at their 3'-encoding ends with the green fluorescent protein (GFP)-expressing tag. All three GFP fusion constructs were expressed under their own promoters (Figure 4A, left panel) and functioned normally (as assayed by their competence to promote exit from rapamycin-induced growth arrest; Figure 4A, right panel). Interestingly, all three fusion proteins predominantly localized to the limiting membrane of the vacuole, which was confirmed by their colocalization with the lipophilic vacuolar membrane dye FM4-64 (Vida and Emr, 1995) (Figure 4B). Consistent with their observed localization to the vacuolar membrane, Ego1-GFP and Ego3-GFP cosedimented largely with the vacuolar alkaline phosphatase (ALP) in the low-speed pellet fraction (Figure 4C). A large part of Gtr2-GFP, however, was lost from this fraction and solubilized readily into the supernatant, indicating that Gtr2 is more weakly associated to the vacuolar membrane than Ego1 and Ego3. (Notably, the levels of Ego1-GFP, Gtr2-GFP, and Ego3-GFP did not dramatically change during the first 3 hr of rapamycin treatment; Figure 4D).

EGO and Rapamycin-Sensitive TOR Complexes Regulate Microautophagy

The vacuoles of EGO mutants, like the ones in wild-type cells, appeared normal during exponential growth and steadily increased in size in response to rapamycin treatment (Figure 5A). This phenotype results from the massive influx of membranous material toward the vacuolar membrane due to the continuous fusion of the outer membranes of macroautophagosomes (Levine and Klionsky, 2004). Accordingly, 3–6 hr following rapamycin treatment, most mutant and wild-type cells harbored almost exclusively one single, enlarged vacuole (Figure 5A). Intriguingly, however, while this process was completely reversed in wild-type cells upon release of the rapamycin block, the vacuoles in *ego1Δ*, *gtr2Δ*, and *ego3Δ* mutants continued to increase in size during the 24 hr recovery period on medium without rapamycin, indicating persistent macroautophagy in these cells (Figure 5A). Therefore, the EGO complex plays a critical role in counterbalancing the influx of membranous material toward the vacuolar membrane.

Current evidence suggests that membrane efflux from the vacuolar membrane can occur by either of two fundamentally different processes, namely microautophagy and retrograde traffic out of the vacuole (Bryant et al., 1998; Dove et al., 2004; Müller et al., 2000). To determine whether the EGO complex mediates microautophagy, we expressed Gtr2 conditionally during the recovery phase from rapamycin treatment. Interestingly, following an induction period of 8 hr on galactose-containing medium, we detected in *gtr2Δ* cells carrying the *GAL1-GTR2* construct, but not in control cells (or in cells expressing *GAL1-GTR2^{Q66L}*; data not shown), the simultaneous establishment of vacuolar membrane invaginations (sometimes occurring concurrently at different sites) leading to the formation and release of small vesicles into the lumen of the vacuole (Figure 5B; similar results were obtained when *GAL1-EGO1* and *GAL1-EGO3* were conditionally expressed

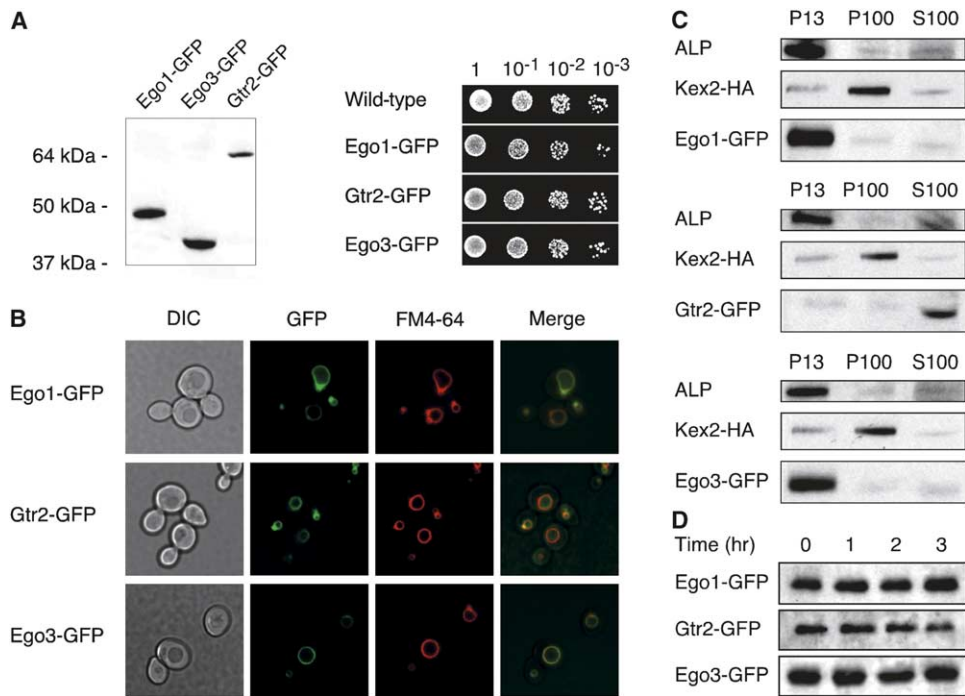


Figure 4. The EGO Complex Localizes to the Limiting Membrane of the Vacuole

(A) Wild-type cells (KT1961) carrying chromosomally tagged *EGO1-GFP* (CDV213), *EGO3-GFP* (CDV214), and *GTR2-GFP* (CDV215) express proteins of 48.2, 46.4, and 66.6 kDa (left panel), respectively, which function normally in permitting exit from rapamycin-induced growth arrest (right panel). For details, see Figure 2G.

(B) Ego1-GFP, Gtr2-GFP, and Ego3-GFP localize to the limiting membrane of the vacuole. Cells (same as in [A]) were labeled with the vacuolar membrane fluorescent dye FM4-64 and the localization of FM4-64 and Ego1-GFP, Gtr2-GFP, and Ego3-GFP was compared by fluorescence microscopy. DIC, differential-interference contrast.

(C) Subcellular fractionation of cells (same as in [A]) expressing Ego1-GFP (upper panel), Gtr2-GFP (panel in the middle), and Ego3-GFP (lower panel), as well as Kex2-HA (pSN222). Exponentially growing cells were made into spheroplasts, lysed by osmotic shock (Dove et al., 2004), and sedimented sequentially to give a 13,000 × g pellet (P13), a 100,000 × g pellet (P100), and a supernatant (S100). Fractions were separated by SDS-PAGE and analyzed by immunoblot analyses using anti-ALP, anti-HA, and anti-GFP antibodies. Kex2-HA and ALP serve as Golgi and vacuolar membrane markers, respectively.

(D) Levels of Ego1-GFP, Gtr2-GFP, and Ego3-GFP following rapamycin treatment (200 ng/ml) for the times indicated were analyzed by immunoblot analysis using anti-GFP antibodies. Equal amounts of total protein were loaded in each lane. Strains (same as in [A]) were grown on YPD medium.

during the recovery phase from rapamycin treatment in corresponding *ego1Δ* and *ego3Δ* mutants, respectively; Figure 5C). These vesicles, which could be released in less than 90 s (Figure 5D), moved freely around the vacuolar lumen indicating that they had fully separated from the vacuolar membrane. Since the formation of these vesicles, which was also observed in wild-type cells recovering from rapamycin treatment (Figure 5B), meets the classical definition of microautophagy, we conclude that the EGO complex is required for the induction of microautophagy during recovery from rapamycin treatment. We could not observe (neither in wild-type nor in *ego* mutant cells) microautophagic vesicle formation during the treatment with rapamycin, and therefore further conclude that TORC1 positively controls microautophagy. This conclusion is supported by the recent finding that rapamycin specifically inhibits microautophagic scission of vesicles into the vacuolar lumen as assayed in a cell-free microautophagy assay (Kunz et al., 2004). Finally, wild-type cells overproducing Gtr2 or Ego3, but not control cells, were competent

to form microautophagic vesicles even in the presence of 50 ng/ml rapamycin (Figure 5E), indicating that the EGO complex acts downstream and/or in parallel of TORC1 to control microautophagy.

We also tested whether the phenotype of an EGO complex mutant may be due to a failure of membrane recycling via the retrograde traffic out of the vacuole. To this end, we determined in both wild-type and *gtr2Δ* cells the localization of an ALP variant (RS-ALP) with an engineered Golgi-retrieval sequence (FXFXD) at its N-terminal region (Bryant et al., 1998). RS-ALP exhibited only the punctate staining pattern that is characteristic of localization to the trans-Golgi network irrespective of either rapamycin treatment or the presence or absence of Gtr2 (Figure 6A). In addition, Golgi membrane-containing cell fractions of exponentially growing wild-type and *gtr2Δ* cells and of corresponding rapamycin treated cells (6 hr) contained both pro-RS-ALP, as well as the proteolytically matured mRS-ALP (data not shown). Thus, the ratio between RS-ALP influx to and retrieval from the vacuolar membrane does not sig-

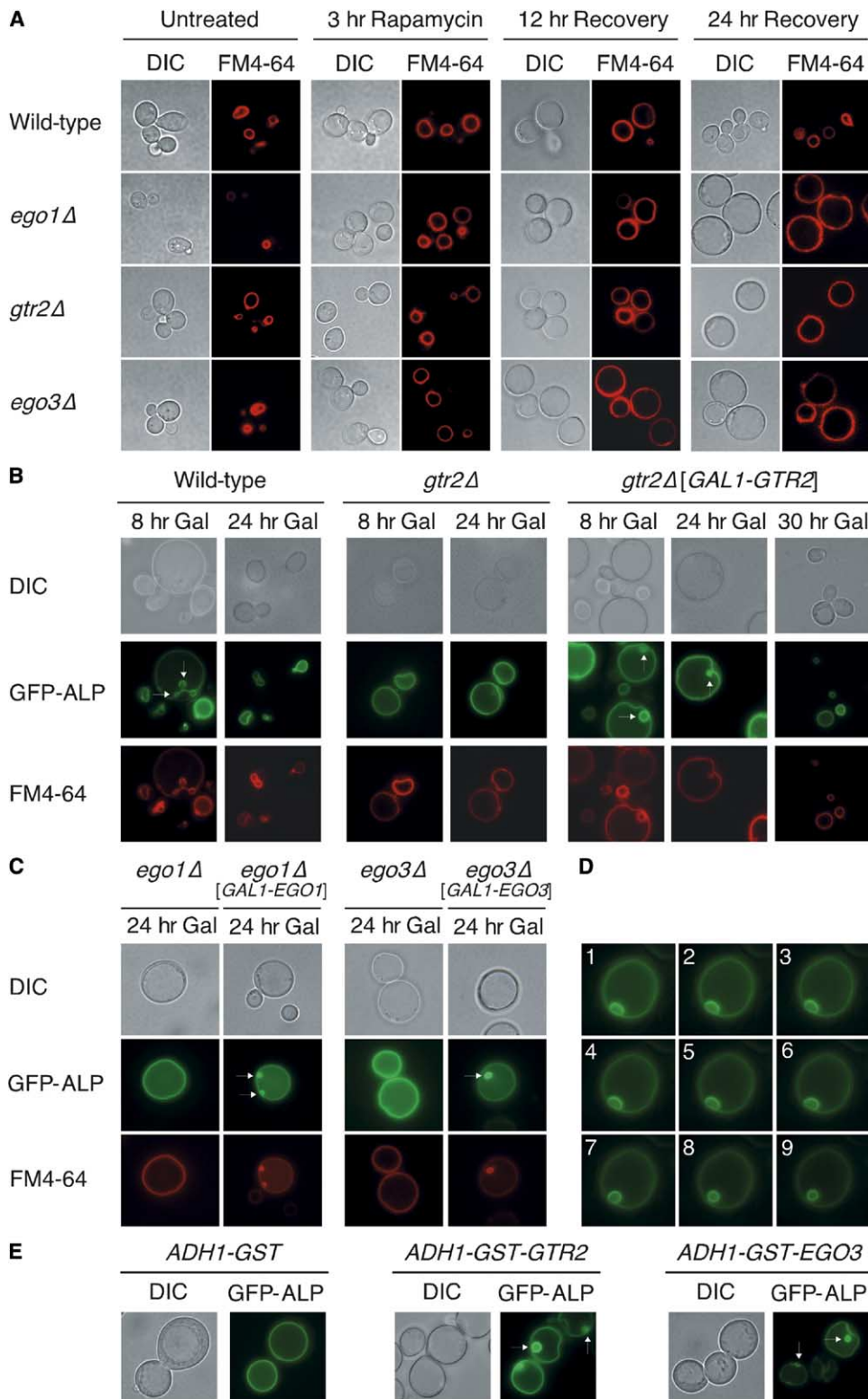


Figure 5. The EGO Complex Triggers Microautophagy during Recovery from Rapamycin Treatment

(A) EGO complex mutants display a single, dramatically enlarged vacuole following release from the rapamycin block. Wild-type (KT1960), *ego1Δ* (CDV210), *gtr2Δ* (CDV212), and *ego3Δ* (CDV211) cells growing exponentially on YPD were treated for 6 hr with rapamycin (200 ng/ml), washed twice, and resuspended in YPD. Cells were labeled with the fluorescent dye FM4-64 before rapamycin treatment (untreated) or following 3 hr of rapamycin treatment, and after 12 and 24 hr of recovery from the rapamycin treatment. For details, see Figure 4B.

(B) Conditional expression of *GTR2* during the recovery phase from rapamycin treatment restores microautophagy. Wild-type (KT1960) and

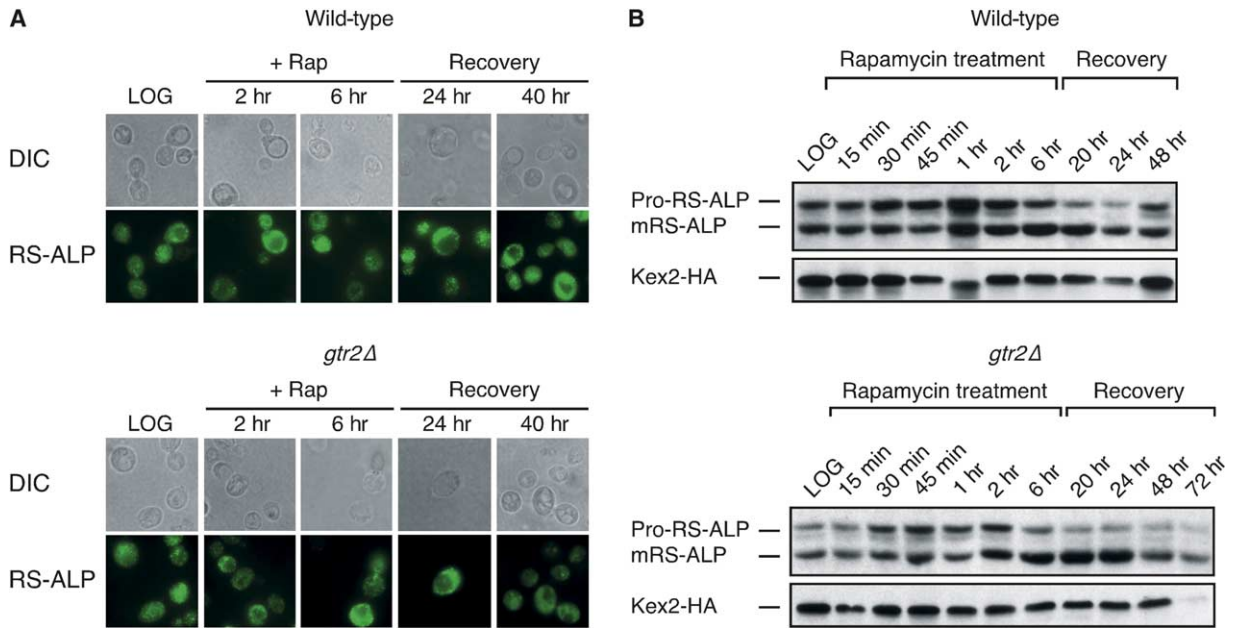


Figure 6. Gtr2 Is Not Required for Retrograde Traffic out of the Vacuole

(A and B) Localization (A) and processing (B) of RS-ALP during exposure to and following recovery from rapamycin treatment. Wild-type (CDV266-1D) and *gtr2Δ* (CDV266-22A) strains bearing plasmids expressing RS-ALP (pSN97) and HA-tagged Kex2 (pSN222) were grown on SD to exponential growth phase (LOG), subjected to a 6 hr rapamycin treatment, washed, and allowed to recover in SD without rapamycin for the indicated times. Localization of RS-ALP was visualized by indirect immunofluorescence (using anti-ALP antibodies) and DIC microscopy (A). Processing of RS-ALP was analyzed by immunoblot analysis using anti-ALP (and anti-HA for visualizing the Golgi membrane marker Kex2-HA; [B]).

nificantly change as a result of TORC1 inhibition and/or loss of Gtr2. During the rapamycin treatment (compare 2 hr versus 6 hr time point; Figure 6B) and during the first 20 hr of recovery from rapamycin treatment, almost the entire pool of preexisting pro-RS-ALP gradually underwent maturation irrespective of the presence or absence of Gtr2 (Figure 6B; notably, general protein synthesis resumes in wild-type cells, but not in *gtr2Δ* cells, after 24 hr of recovery; Figures 2E and 2F). Thus, both influx of pro-RS-ALP to and retrieval of mRS-ALP from the vacuole may operate normally in the presence or absence of TORC1 and/or EGO complex function. Consequently, retrograde traffic out of the vacuole is neither sufficient nor necessary for the recovery from rapamycin-induced growth arrest. This conclusion is supported by our finding that mutants blocking this pathway (e.g., *vac7*, *vac14*, and *svp1* [Bryant et al., 1998; Dove et al., 2004]) normally resume cell

proliferation following release from rapamycin arrest (data not shown).

Large-Scale Genetic Network Analyses of the EGO Complex Identify Glutamine as a Key Metabolite in TOR Signaling

To extend our understanding of EGO complex function, we performed a synthetic genetic array analysis (SGA; see Experimental Procedures). As expected on the basis of the rapamycin-hypersensitivity of *gtr2Δ* cells, *tor1Δ* was found to be synthetically sick when combined with *gtr2Δ* (Figure 7A). In addition, either *rtg2Δ* or *rtg3Δ* mutations, both of which cause serious defects in glutamate/glutamine homeostasis (Butow and Avadhani, 2004), resulted in a synthetic lethal phenotype when combined with *gtr2Δ* that could be reversed by either introduction of a Gtr2-expressing plasmid, or supplementing the medium with glutamate (Figure 7B).

gtr2Δ (CDV212) cells without (*gtr2Δ*) and with the integrative *GAL1-GTR2* (pCDV991) plasmid (*gtr2Δ* [*GAL1-GTR2*]) were grown to exponential phase on SD medium, treated for 6 hr with rapamycin (200 ng/ml), washed twice, and resuspended in SGal/Raf (Gal). To visualize the boundaries of the vacuolar membrane, all strains additionally expressed GFP-ALP (from plasmid pRS426-GFP-ALP). Cells were labeled with the fluorescent dye FM4-64 (after the indicated recovery times on SGal/Raf), and the localization of FM4-64 and GFP-ALP was compared by fluorescence microscopy. White arrows indicate some sites of microautophagic vesicle formation.

(C) Same experiment as in (B) using *ego1Δ* (CDV210 ± *GAL1-EGO1* [pCDV1086]) and *ego3Δ* (CDV211 ± *GAL1-EGO3* [pCDV1085]) mutant cells.

(D) Budding of a microautophagic vesicle into the lumen of the vacuole. The sequence of pictures (covering 90 s in total) was taken from a *gtr2Δ* [*GAL1-GTR2*] cell (see [B] for details) 24 hr following release from rapamycin-containing medium into SGal/Raf. GFP-ALP was visualized as in (B).

(E) Wild-type (CDV147; pRS426-GFP-ALP) cells overexpressing *GTR2* (pCDV1080; *ADH1-GST-GTR2*), or *EGO3* (pCDV1083; *ADH1-GST-EGO3*) from the strong constitutive *ADH1* promoter, but not control cells (carrying pCDV1082; *ADH1-GST*), form microautophagic vesicles in the presence of 50 ng/ml rapamycin. GFP-ALP was visualized as in (B), following a 6 hr rapamycin treatment.

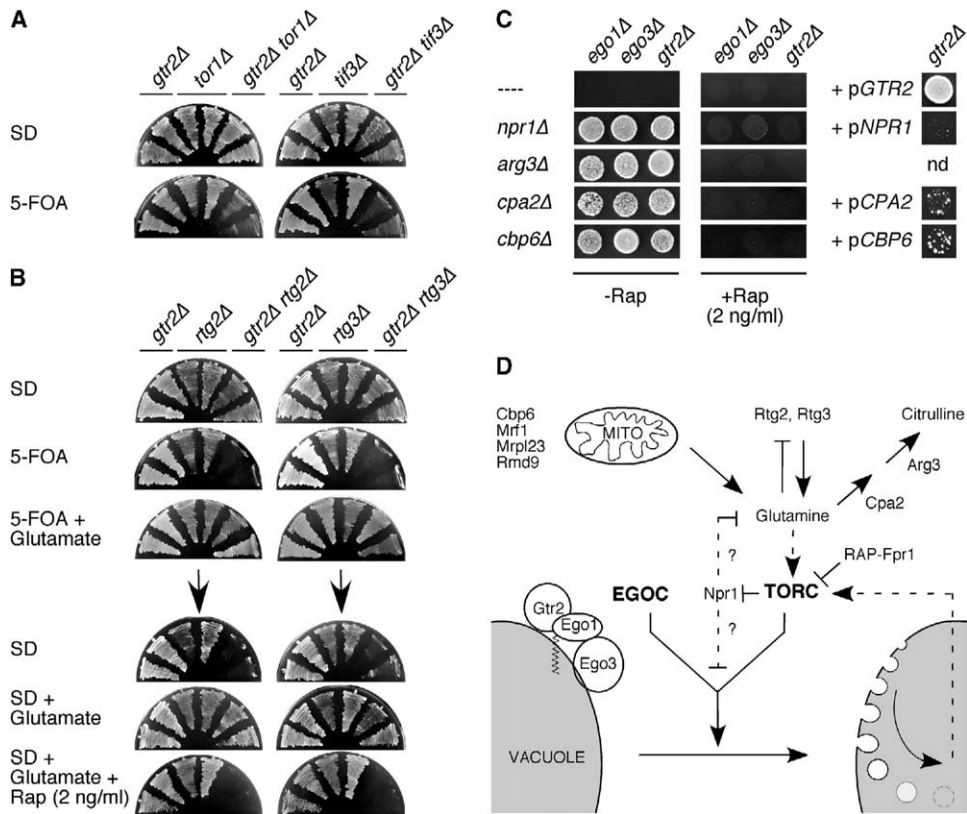


Figure 7. Global Mapping of the *gtr2Δ* Genetic Interaction Network

(A and B) SGA analysis using a *gtr2Δ* strain (CDV209) revealed synthetic sick or lethal interactions with *tor1Δ* and *tif3Δ* (A) or *rtg2Δ* and *rtg3Δ* (B), respectively. To verify the synthetic genetic interactions, original YKO mutants were backcrossed to the *gtr2Δ* strain (CDV209) and the corresponding diploids were transformed with the centromeric YCplac33-*GTR2* plasmid, sporulated, dissected on YPD medium, and streaked on SD plates, SD plates containing 5'-FOA (to select for cells that have lost the *URA3*-containing YCplac33-*GTR2* plasmid) (Boeke et al., 1987), or SD plates containing 5'-FOA plus glutamate (0.2%). The synthetic sick phenotype of the *gtr2Δ tif3Δ* double mutant was also reversed by the expression of Tif3 from a complementing plasmid (data not shown). The relevant genotypes are indicated. In (B), cells growing on plates containing 5'-FOA plus glutamate (0.2%) were subsequently replica-plated on SD, SD-glutamate (0.2%), and SD-glutamate (0.2%) plus rapamycin (2 ng/ml) plates.

(C) Suppressor mutations isolated from the *gtr2Δ* SGA double mutant collection. Original YKO mutants were backcrossed with *ego1Δ* (CDV207), *gtr2Δ* (CDV209), or *ego3Δ* (CDV208) mutants. Spores carrying both mutations were selected and assayed for recovery from rapamycin treatment as in Figure 2G except that recovery was additionally tested on YPD plates containing 2 ng/ml rapamycin. To verify that the suppressive effect is due to the loss of function mutation, selected double mutants were complemented with a plasmid harboring the corresponding wild-type gene and assayed (following growth on SD) for recovery from rapamycin treatment as in Figure 2G.

(D) Schematic pathway depicting the regulation of microautophagy by the TOR and EGO complexes. Arrows and bars denote positive and negative interactions, respectively. Interactions may be direct or indirect as further detailed in the text. Notably, even though we favor the possibility that the Rtg1/2/3-dependent retrograde response pathway acts upstream of TOR (with a presumed positive feedback control mechanism of TOR on glutamine levels; see also Butow and Avadhani, 2004), we presently cannot distinguish it from a model in which retrograde regulation of Rtg1/2/3 in response to decreased glutamate/glutamine levels is via TOR (Crespo et al., 2002). Finally, even though our genetic data favor a model in which glutamine acts as a key nutrient-signaling molecule upstream of TOR, alternative models in which the various suppressor mutations may impinge on TOR via a glutamine-independent mechanism(s) cannot be excluded at present.

Notably, the observed effect of glutamate was strongly dependent on TORC1 function, since it was entirely abolished in the presence of very low, subinhibitory levels of rapamycin (i.e., 2 ng/ml; Figure 7B). These findings indicate that glutamate/glutamine may act upstream of TORC1 and are in accord with the suggestion that the TOR pathway may sense glutamine, among other unknown nutrient compounds (Crespo et al., 2002). This model is further corroborated by the finding of several mutations (isolated in a genome-wide screen for *gtr2Δ* suppressors; see Experimental Procedures) that suppressed the defect in exit from rapamycin-

induced growth arrest of all three EGO mutants (Figures 7C and 7D). These mutations include (1) *cbp6Δ*, *mrf1Δ*, *mrpl23Δ*, and *rmd9Δ*, all of which exhibit severe mitochondrial defects and hence are expected to induce robust Rtg2/3-mediated upregulation of glutamate/glutamine synthesis (Butow and Avadhani, 2004); (2) *cpa2Δ* and *arg3Δ*, which lack carbamoyl-phosphate synthase and ornithine carbamoyl transferase, respectively, that normally remove glutamine by converting it in sequential enzymatic reactions to citrulline; and (3) *npr1Δ*, which causes defects in degradation of amino acid permeases (Schmidt et al., 1998), and which has

recently been reported to slightly increase glutamine levels (Crespo et al., 2004) (an effect that may be more pronounced following rapamycin treatment). Importantly, the suppressive effects of the isolated mutations depended on a fully functional TORC1 complex, as illustrated by the fact that the presence of very low, sub-inhibitory levels of rapamycin (i.e., 2 ng/ml) during the recovery phase (a concentration that does not prevent the recovery from rapamycin treatment of wild-type cells; data not shown) completely abolished the observed suppressive effects (Figure 7C). Taken together, our large-scale genetic analyses converge on glutamine as a key molecule that may act in the TOR signaling pathway upstream of TORC1 (Figure 7D).

Discussion

In a first attempt to unravel the mechanisms that control exit from quiescence, we sought to identify those yeast mutants that are specifically defective in exit from rapamycin-induced growth arrest. Here, we focused our efforts on the characterization of three mutants, namely *ego1Δ*, *gtr2Δ*, and *ego3Δ*, and showed that they are likely defective in the same (EGO) protein complex. Several observations support this conclusion. First, all three mutants exhibit the same defects in both resumption of growth following rapamycin treatment and growth in the presence of subinhibitory rapamycin levels. Second, these defects can be reversed in all three mutants by the same suppressor mutations (including *npr1Δ*, *arg3Δ*, *cpa2Δ*, and *cbp6Δ*). Finally, and most compellingly, the three corresponding gene products colocalize to the vacuolar membrane and interact with each other as assayed by both two-hybrid and classical biochemical coprecipitation experiments.

How is the EGO complex localized to the vacuolar membrane? First, Ego1 is likely to be anchored to the vacuolar membrane via its N-terminal myristoyl group (Ashrafi et al., 1998). Second, Ego3 has a predicted membrane-spanning domain (at position 120–143 of its amino acid sequence; see *S. cerevisiae* genome database, <http://www.yeastgenome.org/>) and may bind PtdIns(3,5)P₂ (Zhu et al., 2001). From these and our own data, we propose the following topology of the EGO complex: (1) Gtr2, which lacks the classical C-terminal lipid modification site that is characteristic to members of the Ras-related GTPase family (Boguski and McCormick, 1993; Nakashima et al., 1999), interacts with Ego1 at the cytoplasmic side of the vacuolar membrane; (2) Ego1 is associated with the vacuolar membrane through its covalently attached N-terminal myristoyl group (and its interaction with Ego3); and (3) Ego3 is anchored in the vacuolar membrane via its presumed membrane-spanning and lipid binding domains (and its interaction with Ego1; Figure 7D). In support of this topology model, we observed that loss of individual components of the EGO complex did not significantly affect the localization of the other two, except for loss of Ego1 that resulted in a partial redistribution of Gtr2-GFP to the cytoplasm (data not shown).

Our current data indicate an essential role of the EGO complex in activation of microautophagy following release from a rapamycin block, a process that is speci-

fically required to counterbalance the massive membrane influx toward the vacuolar membrane resulting from rapamycin-induced macroautophagy. The observation that EGO complex function becomes essential for growth when TORC1 activity is reduced (i.e., in the presence of subinhibitory rapamycin levels or in the absence of Tor1) substantiates this notion. An interesting consequence of this genetic interaction is that mutations, which positively or negatively modulate TORC1 activity, are expected to either alleviate or aggravate, respectively, the defects exhibited by EGO complex mutants. To identify potential regulators of TORC1, we therefore performed a genome-wide screen for mutations that either suppressed the *gtr2Δ* phenotype, or, conversely, resulted in a synthetic lethal/sick phenotype when combined with *gtr2Δ*. As schematically illustrated in Figure 7D, these studies identified a regulatory network of proteins that converges on the amino acid glutamine as a key metabolite in TOR signaling. These findings are in line with those of a previous report (Crespo et al., 2002). Nevertheless, we would like to emphasize that our genetic data allow at present no definite exclusion of alternative models in which the various suppressor mutations may impinge on TORC1 via a glutamine-independent mechanism(s).

An important finding of our present study is that diverse readouts, which are negatively controlled by TORC1 (e.g., glycogen accumulation, phosphorylation of eIF2 α on Ser 51, and macroautophagy; Figures 2B and 2F; and data not shown), depended on the presence of Ego1, Gtr2, and Ego3 during recovery from rapamycin treatment for resetting to their initial status. These data suggest the presence of an EGO complex-mediated positive feedback loop that impinges on TOR itself, which is in line with our finding that overproduction of Gtr2 or Ego3 enhances rapamycin resistance. In further support of this suggestion, a recent study identified Ybr077C/Nir1/Ego3 as the target of an engineered molecule that suppresses the effects of rapamycin, possibly by causing a gain of function of Ybr077C/Nir1/Ego3 (Huang et al., 2004). Importantly, the transcript profile of exponentially growing *ybr077cΔ/nir1Δ/ego3Δ* cells was reported to be strikingly similar to the one of rapamycin-treated wild-type cells, further substantiating a role for Ego3 in TOR activation (Huang et al., 2004).

A formal prediction inferred from our model that the EGO complex activates TOR activity is the existence of mutations that are simultaneously synthetically lethal/sick with either loss of EGO complex function or reduced TOR activity. Interestingly, in this context, our SGA analysis recovered the *tif3Δ* mutant, which meets both of these requirements, i.e., it is hypersensitive to rapamycin (Parsons et al., 2004) and synthetically sick in combination with *gtr2Δ* (Figure 7A). Tif3, the yeast eIF4B homolog, is thought to stimulate eIF4A helicase activity to enhance unwinding of inhibitory secondary structures in the 5' untranslated region of mRNAs. In mammalian cells, eIF4B has been identified as an indirect target of mTOR and suggested to be particularly important for the translation of mRNAs encoding proteins implicated in cell cycle progression (Raught et al., 2004). These data not only indicate that Tif3 may play a critical role in cell proliferation control under condi-

tions of starvation and/or low TOR activity but also further support the notion that the EGO complex positively acts on TOR.

How could the EGO complex-mediated microautophagy be coupled to the control of TOR activity? We speculate that microautophagy reestablishes a balance in the distribution of membranes in the entire endomembranous system and, in parallel, promotes a concentration of the vacuolar amino acid reservoir. Because TOR is localized to distinct membrane-associated protein complexes (Kunz et al., 2000; Wedaman et al., 2003), it is ideally placed to integrate information on the general dynamics of membrane fluxes in the cell. Alternatively, TOR could be implicated in communicating the status of the internal vacuolar nutrient pool. This may be accomplished via Kog1 (the yeast homolog of the mTOR binding partner raptor), which is localized at the vacuolar membrane (<http://yeastgfp.ucsf.edu>) and which may regulate TOR activity in analogy to the situation in animal cells (Kim et al., 2002), possibly in response to the vacuolar amino acids level. In this context, it is intriguing that Sch9, the closest yeast homolog of the mTOR upstream regulatory protein kinase B (PKB/Akt), has recently been localized to the vacuolar membrane as well (Jorgensen et al., 2004). Taken together, while the detailed molecular mechanism by which the EGO complex may regulate TOR awaits further elucidation, our study demonstrates the existence of a new growth control mechanism that originates at the vacuolar membrane.

Experimental Procedures

Strains, Media, and Genetic Techniques

Wild-type strains KT1960, KT1961, CDV147, and EGY48 and the *pho8Δ60* strain TS139 were described earlier (Gyuris et al., 1993; Pedruzzi et al., 2003; Schmelzle et al., 2004). The yeast knockout collection (YKO) wild-type strains BY4741 and Y2922 (MAT α *mfa1Δ::MFA1pr-HIS3 can1Δ his3Δ1 ura3Δ0 lys2Δ0*) were provided by C. Boone (Giaever et al., 2002; Tong et al., 2001). PCR-based gene deletions (*ykr007w/ego1::natMX4*, *gtr2::natMX4*, and *ybr077c/ego3::natMX4* either transformed into Y2922 to create CDV207, CDV209, and CDV208, respectively, or transformed into KT1960 to create CDV210, CDV212, and CDV211, respectively, or transformed into TS139 to create CDV284, CDV286, and CDV285, respectively) and tagging of chromosomal genes (*YKR007W/EGO1-GFP-TRP1*, *GTR2-GFP-TRP1*, and *YBR077C/EGO3-GFP-TRP1* transformed into KT1961 to create CDV213, CDV215, and CDV214, respectively, and *YKR007W/EGO1-myc13-kanMX6* and *GTR2-myc13-kanMX6* transformed into KT1961 to create FD19 and FD21, respectively) were done as described (Longtine et al., 1998). Diploid strains FD24 (*ego1::natMX4/EGO1 GTR2-myc13-kanMX6/GTR2 EGO3-GFP-TRP1/EGO3*) and FD25 (*EGO1-myc13-kanMX6/EGO1 GTR2-GFP-TRP1/GTR2 ego3::natMX4/EGO3*) were constructed by a series of combinatorial mating and sporulation among the isogenic strains CDV210, CDV214, and FD21, and CDV211, CDV215, and FD19, respectively. CDV266-1D (*pho8Δ::kanMX*) and CDV266-22A (*gtr2Δ::natMX4 pho8Δ::kanMX*) are segregants of CDV266, which was created by mating CDV209 and the YKO strain *pho8Δ::kanMX4* (Giaever et al., 2002). Strains were grown at 30°C in standard rich medium (YPD) with 2% glucose or synthetic defined medium (SD) complemented with the appropriate nutrients for plasmid maintenance and either 2% glucose or 2% galactose and 1% raffinose (SGal/Raf) as carbon source (Guthrie and Fink, 1991). Standard genetic manipulations were used (Guthrie and Fink, 1991). Gene deletions were confirmed by phenotypic analyses and/or PCR with gene-specific primers.

Plasmids

Full-length *Ykr007W/Ego1*, *Gtr2*, *Gtr2^{Q66L}* and *Ybr077C/Ego3* were expressed under the control of the *GAL1* promoter from integrative plasmids pCDV1086, pCDV991, pCDV992, and pCDV1085, respectively; N-terminal, GST-tagged versions of full-length *Ykr007W/Ego1*, *Gtr2*, and *Ybr077C/Ego3* were expressed under the control of the *ADH1* promoter from integrative plasmids pCDV1084, pCDV1080, and pCDV1083, respectively; and full-length *Gtr2* and *Gtr2^{Q66L}* were expressed under the control of the *tetO7* promoter from plasmid pVW1009 and pVW1010, respectively. GST was expressed under the control of the *ADH1* promoter from the low copy number plasmid pCDV1082 (*ADH1-GST*). Control plasmids pCM189, YCpIF2, and YCpADH1 were described earlier (Gari et al., 1997; Reinders et al., 1998). To fuse the various genes to the LexA DNA binding domain (DBD) and/or to the activation domain (AD) coding sequences in plasmids pEG202 and pJG4-5 (Gyuris et al., 1993), respectively, *YKR007W/EGO1*, *GTR2*, *YBR077C/EGO3*, and *MSB2* full-length coding sequences were cloned at the polylinker of pJG4-5 and/or pEG202 to yield pJG4-5-*EGO1*, pJG4-5-*GTR2*, pJG4-5-*EGO3*, pJG4-5-*MSB2*, pEG202-*EGO1*, and pEG202-*EGO3*. *Gtr2*, *Cpa2*, and *Cbp6* were expressed under the control of their own promoters from plasmids YCplac33-*GTR2*, *-CPA2*, and *-CBP6*, respectively. Plasmids expressing HA-tagged Npr1 (pAS103), HA-tagged Kex2 (pSN222), RS-ALP (pSN97), and GFP-ALP (pRS426-GFP-ALP) were described previously (Cowles et al., 1997; Nothwehr et al., 1995; Schmidt et al., 1998).

Isolation of EGO Mutants

To identify genes whose products are involved in exit from rapamycin-induced growth arrest, we screened (in duplicate) 4857 viable yeast deletion mutants by arraying strains on YPD plates, replica plating on rapamycin-containing (200 ng/ml) YPD plates followed by incubation for 24 hr at 30°C, and subsequent replica plating on YPD plates (without rapamycin). Of the originally 58 mutants for which both clones assayed exhibited a defect in resumption of growth on the final plates, eight could be confirmed by serial dilution spot assays (using a cut-off value of 100-fold lower colony formation efficiency than wild-type cells; Figure 2G; and data not shown). Notably, all eight mutants were hypersensitive to rapamycin (Figures 2G and 3C; and data not shown).

Immunoblot Analyses and GST Pull-Down

Standard procedures were used for yeast cell extract preparation and immunoblotting (Pedruzzi et al., 2003). Dr. T. Dever kindly provided polyclonal antibodies against eIF2 α . Phosphospecific anti-eIF2 α [pS⁵¹], monoclonal anti-GFP (JL-8), monoclonal anti-HA (HA.11), monoclonal anti-myc (9B11), polyclonal anti-GST, anti-ALP (1D3), and Alexa Fluor® 488 secondary antibodies were purchased from Biosource (Camarillo, CA), BD Biosciences (Palo Alto, TX), Covance (Berkeley, CA), Cell Signaling (Beverly, MA), Covance (Berkeley, CA), Invitrogen, and Molecular Probes (Eugene, OR), respectively. For coprecipitation experiments, GST-tagged Ego1 and Ego3 were purified (using glutathione sepharose beads) from clarified extracts (prepared as in [Lenssen et al., 2005]) of strains FD24 and FD25, respectively, which express the corresponding GST-tagged proteins from integrative plasmids. Bound proteins were eluted with sample buffer (5 min, 95°C) and subjected to standard immunoblot analysis for detection of coprecipitated proteins.

Synthetic Genetic Array Analysis

Synthetic genetic array (SGA) analysis was performed as described (Tong et al., 2001), using a *gtr2Δ* mutant (CDV209) as the bait strain. In total, four double-deletion combinations were found that resulted in a synthetic growth defect and fulfilled the following two criteria: (1) the corresponding YKO single mutant strains (i.e., *tor1Δ*, *tif3Δ*, *rtg2Δ*, and *rtg3Δ*) also exhibited a synthetic growth defect when combined with the dominant negative *Gtr2^{Q66L}* (expressed from pCDV992), and (2) the double-deletion combinations could be complemented as indicated in Figures 7A and 7B. The double mutant collection was also screened for suppressors of the *gtr2Δ*-dependent defect in exit from rapamycin-induced growth arrest. In total, 8 suppressors could be confirmed by the ability of the corresponding YKO single mutants (i.e., *fpr1Δ*, *cbp6Δ*, *mrf1Δ*,

mpr123Δ, *rmc9Δ*, *npr1Δ*, *cpa2Δ*, and *arg3Δ*) to suppress the dominant negative effect of Gtr2^{Q66L} (expressed from pCDV992) with respect to exit from rapamycin-induced growth arrest. The isolation of the FKBP-deficient *fpr1Δ* mutant validated our suppressor screen.

Miscellaneous

Vacuole membranes were visualized *in vivo* by labeling cells with the fluorescent dye FM4-64 (Molecular Probes) and cells were observed by fluorescent microscopy (Vida and Emr, 1995). Indirect immunofluorescence, two-hybrid, and Northern blot were performed as described (Guthrie and Fink, 1991; Lenssen et al., 2005; Pedruzzi et al., 2003). Progression of autophagy was analyzed by the increase of alkaline phosphatase activity in cells expressing Pho8Δ60, a cytosolic proform of the alkaline phosphatase (Noda et al., 1995). Protein synthesis was measured by the incorporation of [³⁵S] Pro-Mix (Amersham Biosciences) into TCA-precipitable material (De Virgilio et al., 1991).

Acknowledgments

We thank Drs. M. Hall, T. Stevens, K. Tatchell, C. Boone, and T. Dever for providing yeast strains, plasmids, and/or antibodies; R. Bisig for technical assistance; and Drs. C. Georgopoulos, P. Linder, and R. Loewith for critical reading of the manuscript. O.D. and C.D.V. are supported by the Swiss National Science Foundation grants FN-31-65403 (to C. Georgopoulos) and 631-062731.00, respectively.

Received: January 13, 2005

Revised: April 18, 2005

Accepted: May 19, 2005

Published: June 30, 2005

References

- Ashrafi, K., Farazi, T.A., and Gordon, J.I. (1998). A role for *Saccharomyces cerevisiae* fatty acid activation protein 4 in regulating protein *N*-myristoylation during entry into stationary phase. *J. Biol. Chem.* **273**, 25864–25874.
- Boeke, J.D., Trueheart, J., Natsoulis, G., and Fink, G.R. (1987). 5-Fluoroorotic acid as a selective agent in yeast molecular genetics. *Methods Enzymol.* **154**, 164–175.
- Boguski, M.S., and McCormick, F. (1993). Proteins regulating Ras and its relatives. *Nature* **366**, 643–654.
- Bryant, N.J., Piper, R.C., Weisman, L.S., and Stevens, T.H. (1998). Retrograde traffic out of the yeast vacuole to the TGN occurs via the prevacuolar/endosomal compartment. *J. Cell Biol.* **142**, 651–663.
- Butow, R.A., and Avadhani, N.G. (2004). Mitochondrial signaling: the retrograde response. *Mol. Cell* **14**, 1–15.
- Cherkasova, V.A., and Hinnebusch, A.G. (2003). Translational control by TOR and TAP42 through dephosphorylation of eIF2 α kinase GCN2. *Genes Dev.* **17**, 859–872.
- Cooper, T.G. (2002). Transmitting the signal of excess nitrogen in *Saccharomyces cerevisiae* from the Tor proteins to the GATA factors: connecting the dots. *FEMS Microbiol. Rev.* **26**, 223–238.
- Cowles, C.R., Odorizzi, G., Payne, G.S., and Emr, S.D. (1997). The AP-3 adaptor complex is essential for cargo-selective transport to the yeast vacuole. *Cell* **91**, 109–118.
- Crespo, J.L., Helliwell, S.B., Wiederkehr, C., Demougin, P., Fowler, B., Primig, M., and Hall, M.N. (2004). NPR1 kinase and RSP5–BUL1/2 ubiquitin ligase control GLN3-dependent transcription in *Saccharomyces cerevisiae*. *J. Biol. Chem.* **279**, 37512–37517.
- Crespo, J.L., Powers, T., Fowler, B., and Hall, M.N. (2002). The TOR-controlled transcription activators GLN3, RTG1, and RTG3 are regulated in response to intracellular levels of glutamine. *Proc. Natl. Acad. Sci. USA* **99**, 6784–6789.
- De Virgilio, C., Piper, P., Boller, T., and Wiemken, A. (1991). Acquisition of thermotolerance in *Saccharomyces cerevisiae* without heat shock protein hsp104 and in the absence of protein synthesis. *FEBS Lett.* **288**, 86–90.
- Dove, S.K., Piper, R.C., McEwen, R.K., Yu, J.W., King, M.C., Hughes, D.C., Thuring, J., Holmes, A.B., Cooke, F.T., Michell, R.H., et al. (2004). Svp1p defines a family of phosphatidylinositol 3,5-bisphosphate effectors. *EMBO J.* **23**, 1922–1933.
- Düvel, K., and Broach, J.R. (2004). The role of phosphatases in TOR signaling in yeast. *Curr. Top. Microbiol. Immunol.* **279**, 19–38.
- Gari, E., Piedrafita, L., Aldea, M., and Herrero, E. (1997). A set of vectors with a tetracycline-regulatable promoter system for modulated gene expression in *Saccharomyces cerevisiae*. *Yeast* **13**, 837–848.
- Giaever, G., Chu, A.M., Ni, L., Connelly, C., Riles, L., Veronneau, S., Dow, S., Lucau-Danila, A., Anderson, K., Andre, B., et al. (2002). Functional profiling of the *Saccharomyces cerevisiae* genome. *Nature* **415**, 387–391.
- Gray, J.V., Petsko, G.A., Johnston, G.C., Ringe, D., Singer, R.A., and Werner-Washburne, M. (2004). “Sleeping beauty”: quiescence in *Saccharomyces cerevisiae*. *Microbiol. Mol. Biol. Rev.* **68**, 187–206.
- Guthrie, C., and Fink, G.R. (1991). *Guide to Yeast Genetics and Molecular Biology* (San Diego: Academic).
- Gyuris, J., Golemis, E., Chertkov, H., and Brent, R. (1993). Cdi1, a human G1 and S phase protein phosphatase that associates with Cdk2. *Cell* **75**, 791–803.
- Hara, K., Maruki, Y., Long, X., Yoshino, K., Oshiro, N., Hidayat, S., Tokunaga, C., Avruch, J., and Yonezawa, K. (2002). Raptor, a binding partner of target of rapamycin (TOR), mediates TOR action. *Cell* **110**, 177–189.
- Hinnebusch, A.G. (1997). Translational regulation of yeast *GCN4*. A window on factors that control initiator-tRNA binding to the ribosome. *J. Biol. Chem.* **272**, 21661–21664.
- Huang, J., Zhu, H., Haggarty, S.J., Spring, D.R., Hwang, H., Jin, F., Snyder, M., and Schreiber, S.L. (2004). Finding new components of the target of rapamycin (TOR) signaling network through chemical genetics and proteome chips. *Proc. Natl. Acad. Sci. USA* **101**, 16594–16599.
- Jacinto, E., and Hall, M.N. (2003). TOR signalling in bugs, brain and brawn. *Nat. Rev. Mol. Cell Biol.* **4**, 117–126.
- Jorgensen, P., Rupes, I., Sharom, J.R., Schnepfer, L., Broach, J.R., and Tyers, M. (2004). A dynamic transcriptional network communicates growth potential to ribosome synthesis and critical cell size. *Genes Dev.* **18**, 2491–2505.
- Kim, D.H., Sarbassov, D.D., Ali, S.M., King, J.E., Latek, R.R., Erdjument-Bromage, H., Tempst, P., and Sabatini, D.M. (2002). mTOR interacts with raptor to form a nutrient-sensitive complex that signals to the cell growth machinery. *Cell* **110**, 163–175.
- Komeili, A., Wedaman, K.P., O’Shea, E.K., and Powers, T. (2000). Mechanism of metabolic control: Target of rapamycin signaling links nitrogen quality to the activity of the Rtg1 and Rtg3 transcription factors. *J. Cell Biol.* **151**, 863–878.
- Kunz, J., Schneider, U., Howald, I., Schmidt, A., and Hall, M.N. (2000). HEAT repeats mediate plasma membrane localization of Tor2p in yeast. *J. Biol. Chem.* **275**, 37011–37020.
- Kunz, J.B., Schwarz, H., and Mayer, A. (2004). Determination of four sequential stages during microautophagy *in vitro*. *J. Biol. Chem.* **279**, 9987–9996.
- Lenssen, E., James, N., Pedruzzi, I., Dubouloz, F., Camerini, E., Bisig, R., Maillet, L., Werner, M., Roosen, J., Petrovic, K., et al. (2005). The Ccr4-Not complex independently controls both Msn2-dependent transcriptional activation - via a newly identified Glc7/Bud14 type I protein phosphatase module - and TFIIID promoter distribution. *Mol. Cell Biol.* **25**, 488–498.
- Levine, B., and Klionsky, D.J. (2004). Development by self-digestion: molecular mechanisms and biological functions of autophagy. *Dev. Cell* **6**, 463–477.
- Loewith, R., Jacinto, E., Wullschlegel, S., Lorberg, A., Crespo, J.L., Bonenfant, D., Oppliger, W., Jenoe, P., and Hall, M.N. (2002). Two TOR complexes, only one of which is rapamycin sensitive, have distinct roles in cell growth control. *Mol. Cell* **10**, 457–468.

- Longtine, M.S., McKenzie, A., III, DeMarini, D.J., Shah, N.G., Wach, A., Brachat, A., Philippsen, P., and Pringle, J.R. (1998). Additional modules for versatile and economical PCR-based gene deletion and modification in *Saccharomyces cerevisiae*. *Yeast* 14, 953–961.
- Magasanik, B., and Kaiser, C.A. (2002). Nitrogen regulation in *Saccharomyces cerevisiae*. *Gene* 290, 1–18.
- Müller, O., Sattler, T., Flotenmeyer, M., Schwarz, H., Plattner, H., and Mayer, A. (2000). Autophagic tubes: vacuolar invaginations involved in lateral membrane sorting and inverse vesicle budding. *J. Cell Biol.* 151, 519–528.
- Nakashima, N., Noguchi, E., and Nishimoto, T. (1999). *Saccharomyces cerevisiae* putative G protein, Gtr1p, which forms complexes with itself and a novel protein designated as Gtr2p, negatively regulates the Ran/Gsp1p G protein cycle through Gtr2p. *Genetics* 152, 853–867.
- Noda, T., Matsuura, A., Wada, Y., and Ohsumi, Y. (1995). Novel system for monitoring autophagy in the yeast *Saccharomyces cerevisiae*. *Biochem. Biophys. Res. Commun.* 210, 126–132.
- Nothwehr, S.F., Conibear, E., and Stevens, T.H. (1995). Golgi and vacuolar membrane proteins reach the vacuole in *vps1* mutant yeast cells via the plasma membrane. *J. Cell Biol.* 129, 35–46.
- Parsons, A.B., Brost, R.L., Ding, H., Li, Z., Zhang, C., Sheikh, B., Brown, G.W., Kane, P.M., Hughes, T.R., and Boone, C. (2004). Integration of chemical-genetic and genetic interaction data links bioactive compounds to cellular target pathways. *Nat. Biotechnol.* 22, 62–69.
- Peduzzi, I., Dubouloz, F., Cameroni, E., Wanke, V., Roosen, J., Winderickx, J., and De Virgilio, C. (2003). TOR and PKA signaling pathways converge on the protein kinase Rim15 to control entry into G₀. *Mol. Cell* 12, 1607–1613.
- Raught, B., Peiretti, F., Gingras, A.C., Livingstone, M., Shahbazian, D., Mayeur, G.L., Polakiewicz, R.D., Sonenberg, N., and Hershey, J.W. (2004). Phosphorylation of eucaryotic translation initiation factor 4B Ser422 is modulated by S6 kinases. *EMBO J.* 23, 1761–1769.
- Reinders, A., Bürckert, N., Boller, T., Wiemken, A., and De Virgilio, C. (1998). *Saccharomyces cerevisiae* cAMP-dependent protein kinase controls entry into stationary phase through the Rim15p protein kinase. *Genes Dev.* 12, 2943–2955.
- Schmelzle, T., Beck, T., Martin, D.E., and Hall, M.N. (2004). Activation of the RAS/cyclic AMP pathway suppresses a TOR deficiency in yeast. *Mol. Cell. Biol.* 24, 338–351.
- Schmidt, A., Beck, T., Koller, A., Kunz, J., and Hall, M.N. (1998). The TOR nutrient signalling pathway phosphorylates NPR1 and inhibits turnover of the tryptophan permease. *EMBO J.* 17, 6924–6931.
- Sekiguchi, T., Hirose, E., Nakashima, N., Ii, M., and Nishimoto, T. (2001). Novel G proteins, Rag C and Rag D, interact with GTP-binding proteins, Rag A and Rag B. *J. Biol. Chem.* 276, 7246–7257.
- Shamji, A.F., Kuruvilla, F.G., and Schreiber, S.L. (2000). Partitioning the transcriptional program induced by rapamycin among the effectors of the Tor proteins. *Curr. Biol.* 10, 1574–1581.
- Tate, J.J., and Cooper, T.G. (2003). Tor1/2 regulation of retrograde gene expression in *Saccharomyces cerevisiae* derives indirectly as a consequence of alterations in ammonia metabolism. *J. Biol. Chem.* 278, 36924–36933.
- Tong, A.H., Evangelista, M., Parsons, A.B., Xu, H., Bader, G.D., Page, N., Robinson, M., Raghibizadeh, S., Hogue, C.W., Bussey, H., et al. (2001). Systematic genetic analysis with ordered arrays of yeast deletion mutants. *Science* 294, 2364–2368.
- Vida, T.A., and Emr, S.D. (1995). A new vital stain for visualizing vacuolar membrane dynamics and endocytosis in yeast. *J. Cell Biol.* 128, 779–792.
- Wedaman, K.P., Reinke, A., Anderson, S., Yates, J., 3rd, McCaffery, J.M., and Powers, T. (2003). Tor kinases are in distinct membrane-associated protein complexes in *Saccharomyces cerevisiae*. *Mol. Biol. Cell* 14, 1204–1220.
- Zhu, H., Bilgin, M., Bangham, R., Hall, D., Casamayor, A., Bertone, P., Lan, N., Jansen, R., Bidlingmaier, S., Houfek, T., et al. (2001). Global analysis of protein activities using proteome chips. *Science* 293, 2101–2105.